Japanese Journal of Applied Physics
Vol. 46, No. 3B, 2007, pp. 1328–1332

Organic Bifunctional Devices with Emission and Sensing Abilities

Hiroyuki OKADA*, Shigeki NAKA, Yohsuke MATSUSHITA, Hiroyuki SHIMADA, Junya YANAGI, Miki SHIBATA, and Hiroyoshi ONNAGAWA

Graduate School of Science and Engineering, University of Toyama, 3190 Gofuku, Toyama 930-8555, Japan

(Received July 7, 2006; accepted September 18, 2006; published online March 16, 2007)

Organic bifunctional devices with emission and sensing abilities were reviewed and a prototype of a matrix was demonstrated. There are two types of device structure: a *bi-function matrix array* (Bi-Matrix) with a stacked layer of organic light-emitting diode (OLED) and organic photodiode (OPD) matrix arrays, and a *multi-function diode* (MFD) which has a structure similar to that of conventional OLED and has two functions of emission and photosensing. For the Bi-Matrix, independent operations of emission and photosensing were achieved; the maximum luminance of its OLED was 77,400 cd/m^2 and the ratio of photoconductivity to dark conductivity was 1×10^4. A prototype 4×4 Bi-Matrix was also demonstrated. For the MFD, a special organic material, the pyrazoline derivative, was used. The highest luminance obtained was 9,270 cd/m^2 under a forward bias condition. The highest photocurrent density was 71 μA/cm^2 and the highest ratio of photo- to dark-conductivity was 1×10^4 under a reverse-bias condition. Details of the prototype 16×16 MFD matrix were also described.
[DOI: 10.1143/JJAP.46.1328]

KEYWORDS: organic light-emitting diode, organic photodiode, matrix array, bi-function

1. Introduction

Organic devices, such as high-efficiency organic light-emitting diodes (OLEDs)[1,2] and organic photodiodes (OPDs),[3,4] are now widely studied because of their merits of being feasible for large area production, ultrathin, lightweight and flexible. The applications of organic devices are various and a new market for such devices will be developed, for example, in flexible displays, electronic papers and RFID tags. Stacked organic device structures of multiphoton emission device,[5,6] tandem-type organic solar cell,[7,8] dual-drive and -emission panel[9] and bi-function matrix array (Bi-Matrix)[10] have also been reported. In this study, first, we describe the Bi-Matrix with a stacked layer of OLED and OPD matrix arrays.[10] Second, we show a special low-molecular-weight organic material the pyrazoline derivative, which has both functions of luminescence and photosensing using a single-stacked device, called a multi-functional diode (MFD). We also optimize the device structure and operation of a 16×16 matrix panel.

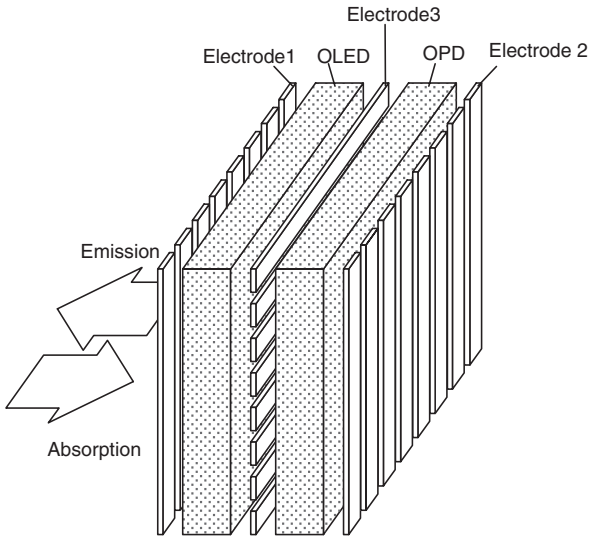

Fig. 1. Basic concept of Bi-Matrix.

2. Experimental Procedure

Figure 1 shows the basic concept of the Bi-Matrix. Electrodes 1 and 3 are transparent and electrode 2 has reflective characteristics. For OLED operation, emission could be observed through the glass substrate. For image sensing operation, the light absorption of the OPD is carried out through the OLED, i.e., a transparent organic light-emitting diode (TOLED)[11] is employed. Figure 2 also shows the basic concept of the MFD. The device structure of a conventional MFD is similar to the stacking layer of the OLED. However, the special material of the pyrazoline derivative exhibits both luminescence and photosensing abilities. The degree of spectrum overlapping between emission and absorption has to be small because of independent operation of the emission and the absorption. For MFD operation, we explored many organic materials and encountered the pyrazoline derivative 4-[2-[5-[4-(diethylamino)phenyl]-4,5-dihydro-1-phenyl-1*H*-pyrazol-3-yl]-ethenyl]-*N*,*N*-diethylaniline (PPR), a hole transport material.[12] The photoluminescence (PL) and absorption spectra of PPR were measured, and are shown in Fig. 3. It was estimated that the fluorescence quantum yield of PPR is almost equal to that of tris(8-hydroxyquinoline) aluminum (Alq_3) from a comparison of the PL intensities of both compounds, and that the absorption coefficient of PPR is much larger than that of Alq_3. Therefore, PPR is suitable for luminescence and light absorption studies.

Figure 4 shows the organic materials under study. To demonstrate Bi-Matrix operation, the device structure indium–tin oxide (ITO)/*N*,*N*′-bis(3-methylphenyl)-(1,1′-biphenyl) 4,4′-diamine (TPD) (50 nm)/Alq_3 (50 nm)/copper phthalocyanine (CuPc)[13] (5 nm)/sputtered indium–zinc oxide (IZO, Idemitsu Kosan)/TPD (100 nm)/*N*,*N*′-ditridecyl-3,4,9,10-perylene-tetracarboxylic diimide (td-PTC) (50 nm)/Al (Device A) was fabricated. To reduce the degree of sputtering damage, we inserted a thin CuPc layer between Alq_3 and IZO. This CuPc layer also acts as an electron injection layer. To reduce series resistance, the device

*E-mail address: okada@eng.u-toyama.ac.jp

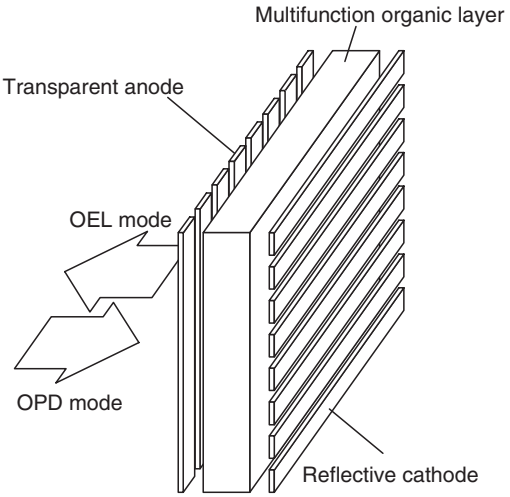

Fig. 2. Basic concept of MFD.

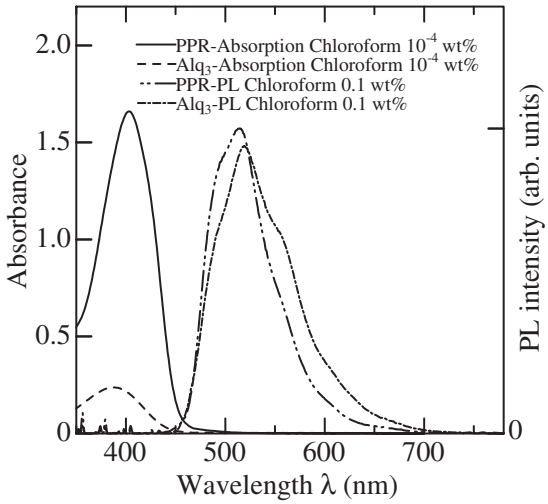

Fig. 3. Photoluminescence and absorption spectra of PPR and Alq_3.

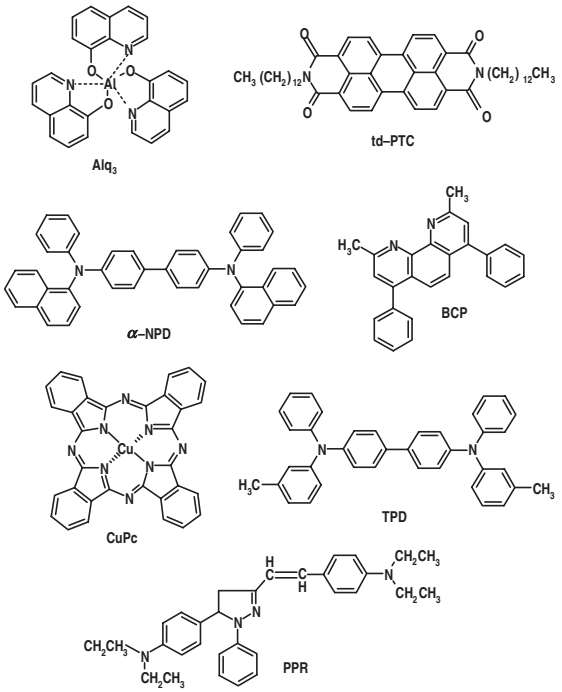

Fig. 4. Organic materials under study.

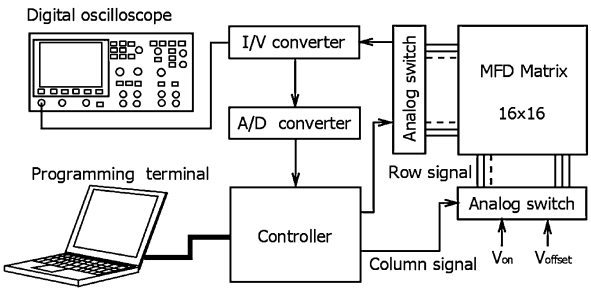

Fig. 5. Measurement system of 16 × 16 MFD panel.

structure ITO/TPD (50 nm)/Alq_3+coumarin 6 (C6) (Alq_3 : C6 = 100 : 1) (50 nm)/LiF (1 nm)/AlNd (15 nm)/MoO_3 (30 nm)/TPD (100 nm)/td-PTC (50 nm)/Al (Device B) was also evaluated. On the other hand, to demonstrate MFD operation, the structure IZO/CuPc (30 nm)/PPR (50 nm)/2,9-dimethyl-4,7-diphenyl-1,10-phenanthroline (BCP)[14] (20 nm)/lithium fluoride (LiF) (1 nm)/Al (Device 1) or PPR (50 nm)/Alq_3[13] (50 nm)/LiF (1 nm)/Al (Device 2) was subsequently evaporated. PPR was dissolved in solvents, such as chloroform and tetralin. Therefore, another device structure of spin-coated (TPD)[13] : PPR = 20 : 80 (1 wt %, chloroform) was used to evaluate a solution-processed device. The device structure under study was IZO/TPD+PPR (110 nm)/BCP (20 nm)/LiF (1 nm)/Al (Device 3).

A xenon (Xe) light source was used to measure the OPD characteristics. The external drive circuit for the prototype 4 × 4 Bi-Matrix and MFD used was a field-programmable gate array (FPGA) (Altera, university program design laboratory kits). The measurement system for the 16 × 16 MFD panel is shown in Fig. 5. The system was composed of a programming terminal with a parallel port, a device controller of a one-chip microcomputer with a 10-bit analog-to-digital (A/D) converter (PIC16F877, Microchip), an analog switch and a current-to-voltage (I/V) converter. The program of this system control was written using Visual Basic (Microsoft). To ensure successful A/D conversion, an input voltage of several volts is necessary; the photocurrent of the MFD was at most 100 nA. To measure the photocurrent of the 16 × 16 MFD panel within 3 s, each pixel has to be measured within 10 ms or less. Therefore, we used an I/V converter with a feedback resistance of 1 MΩ and two stages of a noninversion amplifier with a gain of 20; a universal gain was also set at 20 mV/nA. The time constant of the integration circuit was 8 ms.

3. Results and Discussion

3.1 Bi-Matrix operation

Figures 6 and 7 show the current density (J) vs voltage (V) and luminance (L) vs V characteristics, respectively, of the stacked OLED. For Device A, a maximum luminance (L_{max}) of 1,290 cd/m^2 was obtained. This luminance was one-third that of the TOLED that has been reported to date.[11] However, this can be improved by changing the combination of organic materials and device structures of ITO/CuPc (5 nm)/α-NPD (50 nm)/Alq_3+C6 (Alq_3 : C6 = 100 : 1) (50 nm)/CuPc (5 nm)/IZO, in which L_{max} improved to 3,460 cd/m^2.[15,16] For Device B, series resistance im-

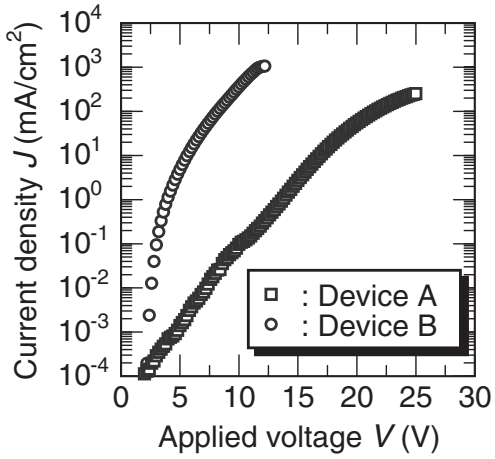

Fig. 6. *J–V* characteristics of OLED for Bi-Matrix.

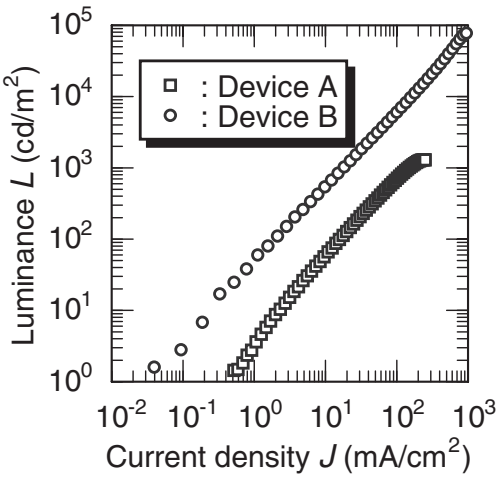

Fig. 7. *L–J* characteristics of OLED for Bi-Matrix.

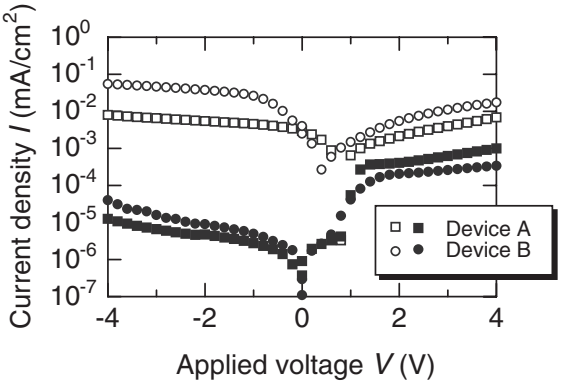

Fig. 8. *J–V* characteristics of OPD for Bi-Matrix.

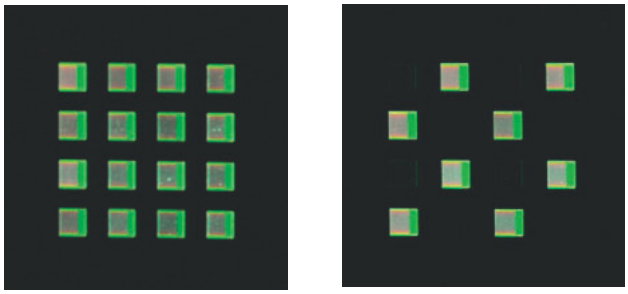

(a) (b)

Fig. 9. Emission pattern of Bi-Matrix: (a) full pattern and (b) checked pattern.

proved, as shown in Fig. 6, and L_{max} also markedly improved to 77,400 cd/m^2, at which the maximum power efficiency of Device B was 5.1 lm/W. The reasons for these improvements are the use of AlNd, the addition of C6 and the insertion of a LiF layer.

Figure 8 shows the experimentally obtained *J–V* characteristics of the stacked OPD. The open symbols and filled symbols show the *J–V* characteristics under illuminated and dark conditions, respectively. The ratios of photoconductivity to dark conductivity (σ_R) of Devices A and B were 10^3 and 10^4 at -2 V, respectively. For the device with a thin TPD layer of 50 nm, the device characteristics were identical. Therefore, a TPD layer of 100 nm is effective for reducing the degree of electric breakdown.

To demonstrate Bi-Matrix operation, a prototype 4×4 Bi-Matrix was fabricated. Figure 9 shows the emission patterns of the OLED operation of the Bi-Matrix. It is obvious that a clear emission is obtained. Figure 10 shows the (a) OPD driving scheme and (b) typical operation point of the Bi-Matrix. The basic driving scheme is similar to that described by Yu and Cao.[17] In this operation, column 1 is selected and columns $2-N$, where N is the number of matrix lines, are not selected. The selected voltage V_{on} and the nonselected voltage V_{offset} were applied, as shown in Fig. 10. In this case, the total current flow is the sum of those in the corresponding columns. The minimum photocurrent I_P and the maximum dark current I_D are expressed as

$$I_D = I_{s\text{-}D} + (N-1) \times I_{ns\text{-}P}, \quad (1)$$

$$I_P = I_{s\text{-}P} + (N-1) \times I_{ns\text{-}D}, \quad (2)$$

where, $I_{s\text{-}P}$ and $I_{s\text{-}D}$ are the photo current and dark current at the selected points, and $I_{ns\text{-}P}$ and $I_{ns\text{-}D}$ are the photo current and dark currents at the nonselected points, respectively. Therefore, the maximum number of capable driving columns, N_{max}, is achieved at $I_P/I_D = 1$. From the experimental data in Fig. 8, N_{max} was estimated to be 259. However, the N_{max} estimated using the 4×4 Bi-Matrix was 19. The experimental N_{max} estimated using the stacked single device was different from that in the case of the 4×4 Bi-Matrix because the *J–V* characteristics of individual devices, particularly I_D and the resultant V_{offset}, exhibit large deviations due to charge accumulation at the electrode/organic and organic/organic interfaces and in the organic layer itself. Figure 11 shows (a) the measurement system for Bi-Matrix operation and (b) the observed currents. In Fig. 11(b), numeric values indicate the observed currents at the selected points. A clear check pattern with on and off currents could be observed.

3.2 *MFD operation*

Figure 12 shows *J–V* and *L–V* characteristics of the Devices 1, 2 and 3. In Device 1, L_{max} was 9,270 cd/m^2. The highest luminance with a high EL efficiency was confirmed in Device 1. In Device 2, L_{max} was 1,750 cd/m^2. The emission characteristics of Device 2 were inferior to those Device 1. This discrepancy is mainly due to removal of the

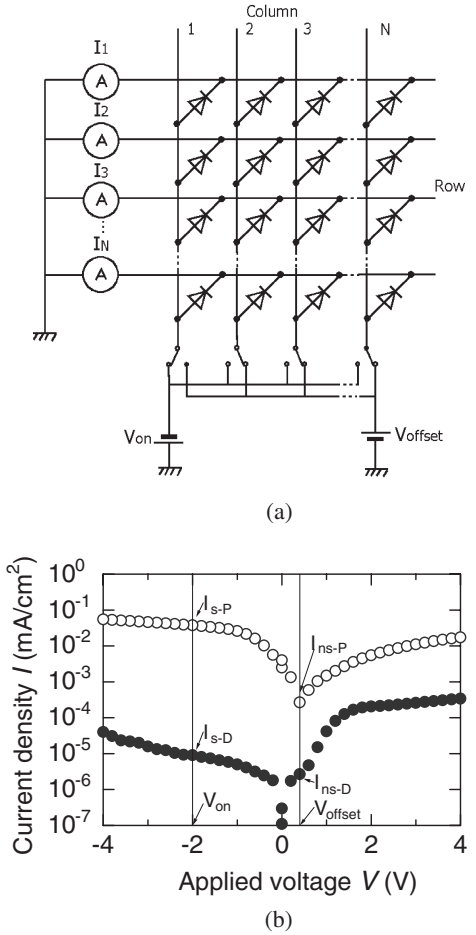

Fig. 10. Operational concept of Bi-Matrix: (a) driving scheme and (b) operation point.

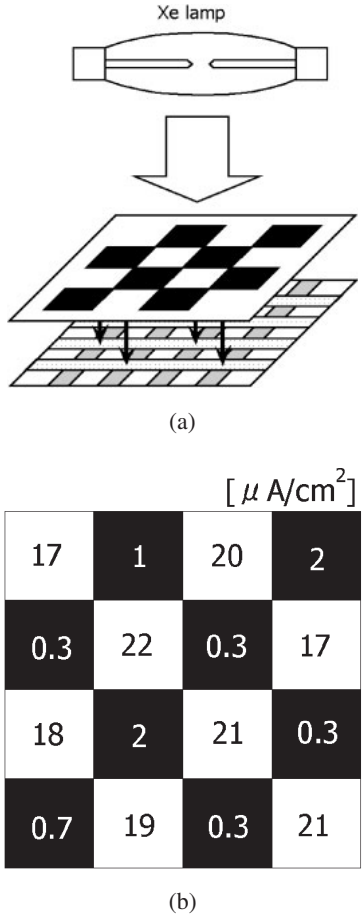

Fig. 11. Detected pattern of Bi-Matrix: (a) measurement system and (b) measured values.

CuPc layer. In Device 3, L_{max} was 3,660 cd/m^2. In this solution-processed device (Device 3), reasonable emission characteristics were also obtained even though the residual solvent might have degraded device characteristics.

Figure 13 shows the J–V characteristics of the OPD. The open circles, squares and triangles and filled circles, squares and triangles show the J–V characteristics under illumination and dark conditions, respectively. In Device 1, at a voltage of -4 V, J_{photo} and σ_R were 15 μA/cm^2 and 2×10^3, respectively. In Device 2, at a voltage of -4 V, J_{photo} and σ_R were 71 μA/cm^2 and 5.4×10^4, respectively. For comparison, the luminance of Device 1 was higher than that of Device 2 owing to higher amount of hole injection in CuPc. In Device 2, however, the photocurrent is one magnitude larger than that of Device 1. It is considered that carrier confinement occurs well at the CuPc/PPR interface. There are no differences between evaporation-processed Device 1 and solution-processed Device 3. Compared with that of another device structure,[18] the photocurrent of Device 3 is one order magnitude smaller than that of a typical device structure.[4]

To demonstrate matrix panel operation, a prototype device of a 16×16 matrix with a Device 1 structure was fabricated. The panel area was 70×70 mm^2. Figure 14 shows the full emission pattern of OLEDs. Figure 15 shows an example of an output waveform of a detected signal. The scanning period of each pixel was 40 ms. The response time of each pixel was approximately 10 ms. This response time

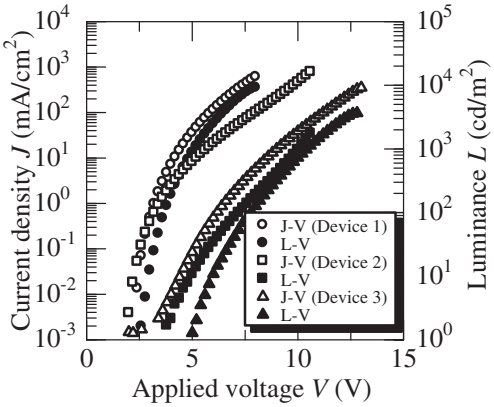

Fig. 12. J–V and L–V characteristics of MFD (OLED mode).

was due to the response time of the measurement circuit. Therefore, the response time of the matrix panel will be operated within 5 ms or less. In particular, in the first signal, there are large fluctuations. These are the issues we investigated. However, a clear output waveform was obtained. Figures 16(a) and 16(b) show the measured currents and detected patterns, respectively. A checked pattern with on and off currents was observed. From Fig. 13, the estimated N_{max} was as large as 267. This large N_{max} was due to the small dark current and small extent of carrier accumulation of this device structure because of the hysteresis of J–V characteristics.

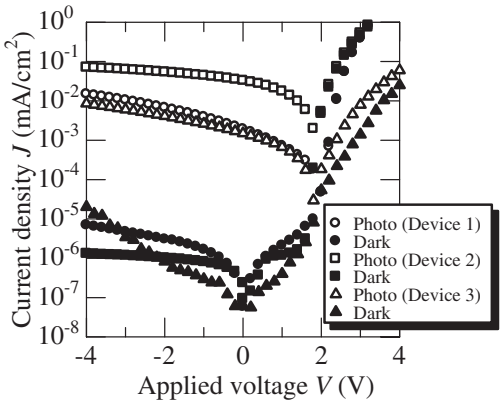

Fig. 13. *J–V* characteristics of MFD (OPD mode).

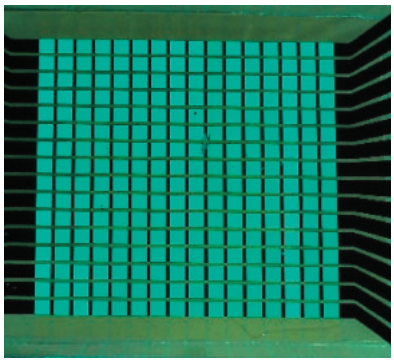

Fig. 14. Emission pattern of MFD.

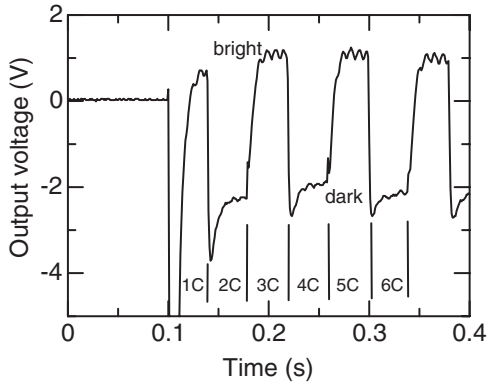

Fig. 15. Output waveform of detected signal.

4. Conclusions

We reviewed the operations of the Bi-Matrix and MFD. For the Bi-Matrix, independent operations of emission and photosensing were achieved for a stacked device and a 4 × 4 matrix array. For MFD, the pyrazoline derivative was useful for achieving both emission and photosensing operations in a single device structure and a 16 × 16 matrix array. Our aim is to apply these panels in an ultralightweight hand-held emission panel with a scanner.

Acknowledgments

This work was partly supported by Innovation Plaza Tokai, Japan Science and Technology Agency.

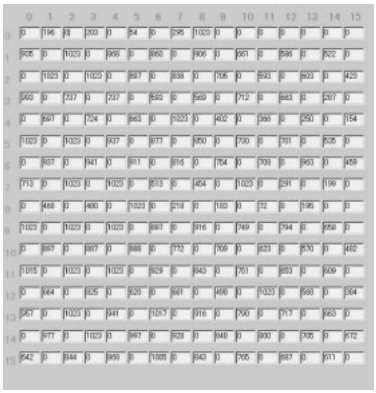

(a)

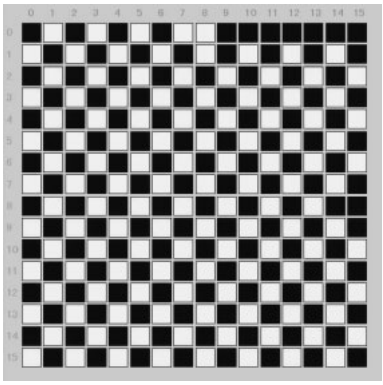

(b)

Fig. 16. OPD operation of prototype 16 × 16 MFD: (a) measured photo current and dark current and (b) detected patterns.

1) C. W. Tang and S. A. VanSlyke: Appl. Phys. Lett. **51** (1987) 913.
2) T. Tsutsui: MRS Bull. **22** (1997) 39.
3) G. Yu, C. Zhang, and A. J. Heeger: Appl. Phys. Lett. **64** (1994) 1540.
4) G. Yu, K. Pakbaz, and A. J. Heeger: Appl. Phys. Lett. **64** (1994) 3422.
5) J. Kido, T. Matsumoto, T. Nakada, J. Endo, K. Mori, N. Kawamura, and A. Yokoi: SID Int. Symp. Dig. Tech. Pap. **34** (2003) 964.
6) L. S. Liao, K. P. Klubek, and C. W. Tang: Appl. Phys. Lett. **84** (2004) 167.
7) K. Triyana, T. Yasuda, K. Fujita, and T. Tsutsui: Jpn. J. Appl. Phys. **43** (2004) 2352.
8) A. Yakimov and S. R. Forrest: Appl. Phys. Lett. **80** (2002) 1667.
9) T. Miyashita, S. Naka, H. Okada, and H. Onnagawa: Jpn. J. Appl. Phys. **44** (2005) 3682.
10) Y. Matsushita, H. Shimada, T. Miyashita, M. Shibata, S. Naka, H. Okada, and H. Onnagawa: Jpn. J. Appl. Phys. **44** (2005) 2826.
11) G. Parthasarathy, P. E. Burrows, V. Khalfin, V. G. Kozlov, and S. R. Forrest: Appl. Phys. Lett. **72** (1998) 2138.
12) H.-J. Yuh, D. Abramsohn, and M. Stolka: Philos. Mag. Lett. **55** (1987) 277.
13) C. Hosokawa, H. Higashi, H. Nakamura, and T. Kusumoto: Appl. Phys. Lett. **67** (1995) 3853.
14) C. Adachi, M. A. Baldo, and S. R. Forrest: J. Appl. Phys. **87** (2000) 8049.
15) G. Parthasarathy, C. Adachi, P. E. Burrows, and S. R. Forrest: Appl. Phys. Lett. **76** (2000) 2128.
16) S. Tabatake, S. Naka, H. Okada, H. Onnagawa, M. Uchida, T. Nakano, and K. Furukawa: Jpn. J. Appl. Phys. **41** (2002) 6582.
17) G. Yu and Y. Cao: U.S. Patent Application Publication, US2002-0017612 (2002).
18) H. Shimada, S. Naka, H. Okada, and H. Onnagawa: Jpn. J. Appl. Phys. **44** (2005) 2830.